VOL. 16, NO. 11, JUNE 2021 ISSN 1819-6608
ARPN Journal of Engineering and Applied Sciences

www.arpnjournals.com

IMPACT OF THERMAL RADIATION AND CHEMICAL REACTION ON MHD HEAT AND MASS TRANSFER CASSON NANOFLUID FLOW PAST A STRETCHING SHEET IN PRESENCE OF HEAT SOURCE/SINK

Nalivela Nagi Reddy[1], Vempati Srinivasa Rao[2] and B. Ravindra Reddy[3]
[1]Department of Mathematics, Geethanjali College of Engineering and Technology, Hyderabad, Telangana, India
[2]Department of Mathematics, Anurag University, Hyderabad, Telangana, India
[3]Department of Mathematics, JNTUH College of Engineering Hyderabad, Hyderabad, India
E-Mail: nagireddynalivela@gmail.com

ABSTRACT

The purpose of present study is to analyse the influence of chemical reaction on MHD Casson nanofluid flow on an elongating sheet taken into the account of radiation and heat absorption/generation. The governing nonlinear PDE's are changed into a nonlinear ODE's by using similarity transformations. The converted equations are solved using numerical technique is notable as Keller box method. The consequence of heat source/sink, Prandtl number, Casson parameter, magnetic field, Brownian motion, thermophoresis, thermal radiation and chemical reaction parameters on velocity, temperature, and concentration profiles are depicted and elucidate in physical terms. A resemblance with previously issued results shown a perfect agreement. Numerical values of physical quantities, such as velocity gradient, heat transfer rate and the mass transfer rate are arranged in tabular form.

Keywords: thermal radiation, heat source/ sink, stretching sheet, casson nanofluid, MHD, chemical reaction.

INTRODUCTION

The study of nanofluids have fascinated because of its remarkable applications in industry such as solar cells, electronics, solar stills, communication, solar cooling systems, computing technologies, solar collectors, optical devices, water heaters, lasers, absorption refrigeration systems, and medicine, synthesis of various solar devices because of their higher properties over the conventional fluids. A nanofluid, consisting of a base fluid and nanoparticles, is a modern division of heat transfer fluids. The utilization of supplement is an approach to intensify the performance of heat transfer in base fluids. The heat conductance of conventional heat transfer fluids does not encounter the demands of modern cooling rate. Nanofluids are suspensions of ultrafine-grained solid particles (nanoparticles) and it improves the convective heat transfer and heat conductivity in common fluids. Choi and Eastman [1] analysed the increased thermal conductivity of nanoparticle fluids. S. K. Das *et al.* [2] investigated the Heat Transfer in Nanofluids. Natural convective heat and mass transfer nanofluid boundary layer flow through a vertical plate with convective boundary condition was studied by Aziz and W.A. Khan [3]. D. Srinivasacharya and Ontela Surender [4] examined the non-similar solution by considering double stratification on natural convection heat transfer of a nanofluid in a porous saturated medium over a vertical plate. Elsheikh *et al*. [5] studied the various applications in solar energy with nanofluids.

Magnetohydrodynamic (MHD) nanofluids perform an important part in several manufacturing procedures such as in hybrid fuel generation, modulator, economy fuel in modern power generation plants, gratings, coolant in continuous metallurgical sheets, fiber filters, vehicle cooling, loud speakers, plastic sheet extrusion and processes of polymers, and magnetic cells, etc. Rizwan Ul Haq *et al*. [6] analysed the magneto-hydrodynamic stagnation point Nanofluid flow in presence of radiation on a stretching sheet with slip conditions. A.S. Dogonchi *et al*. [7] discussed heat transfer and thermal radiation MHD nanofluid flow between parallel plates. A. Kamran *et al.* [8] observed Magneto-hydrodynamic Casson Nanofluid with velocity slip and Joule heating. Jawad Raza *et al.,* [9] investigated MHD heat and mass transfer Nanofluid flow past a nonlinear permeable stretching sheet with multiple slips. Saeed Islam *et al*. [10] examined the influence of thermal radiation and hall current between two surfaces on MHD micropolar non-Newtonian hybrid Nanofluid flow.

Thermal radiation plays an important role in dissipating heat from the surface. It has applications in manufacturing industries such as chopper, space vehicles, reliable equipment design, satellites, atomic furnaces, missiles, space technology and procedures related to high temperature. Yanala Dharmendar Reddy *et al*., [11] analyzed thermal radiation and suction effects on MHD Nanofluid boundary layer flow on a non-linear stretching sheet. Kothandapani and J. Prakash [12] observed peristaltic transport in a tapered asymmetric channel of a Williamson Nanofluid in the presence of thermal radiation. C.Sulochana *et al*. [13] analysed effects of soret and suction/blowing on MHD stagnation point flow of a radiative Carreau nanofluid on a stretching surface. Yap Bing Kho *et al*., [14] investigated impact of radiation on MHD heat and mass transfer Casson Nanofluid flow on a porous stretching sheet. Jawad Raza [15] discussed impact of radiation and velocity slip on magnetohydrodynamic stagnation point flow of Casson fluid with convective boundary conditions through a linear elongated sheet.

Combined heat and mass transfer flows in the existence of chemical reaction have innumerable applications in engineering, for instance energy transfer in a desert cooler, nuclear reactor safety, evaporation, combustion systems, extrusion of polymer drying, solar collectors, chemical coating of flat plates, metallurgy, manufacturing of ceramics, hot rolling, chemical engineering, polymer production and food processing. Some researchers have been investigated in this region. Manjula Jonnadula *et al*. [16] studied chemical reaction effect on MHD heat and mass transfer boundary layer flow past a stretching sheet. Tasawar Hayat *et al*., [17] analysed Magnetohydrodynamic nanofluid stretched flow with chemical reaction and power-law velocity. N. Pandya *et al*., [18] investigated effect of Chemical reaction, Radiation, Soret and Dufour on unsteady MHD dusty fluid flow through inclined porous plate embedded in porous medium. Sajid Qayyum *et al.,* [19] observed impact of Newtonian stagnation point flow on magnetohydrodynamic Walters-B nanofluid with chemical reaction, heat and mass transfer conditions. Sreedhar G. and Rama Bhupal Reddy B. [20] investigated in presence of Chemical Reaction through an infinite porous vertical plate on unsteady MHD flow with heat Absorption.

The study of heat generation/absorption parameter on the moving fluid is influential in sight of diverse physical problems. Uneven heat generation plays crucial part in heat dissipation problems. With the accelerated development of electronic technology, efficient cooling of electronic equipment has evolved to cool a variety of electronic equipment and is provided by separate transistors for mainframes and power supplies for telephone switches. The influence of the heat generation/absorption plays a crucial role in the heat efficiency of base fluids. Its pertinence is seen in the heat discharge of nuclear fuel residues, food storage, the production of plastic and rubber sheets, motion of fluids in fixed bed reactors and much more. Kumar and Singh [21] investigated impact of heat source/sink on MHD steady laminar boundary layer natural convective flow through a concentric annulus region directed vertically. Heat transfer, radiation, and heat source/sink effects on visco-elastic fluid on a stretching surface were analysed by Cortell [22]. Heat source and chemical reaction impact on MHD flow past a moving vertical plate with convective surface conditions are analysed by Dharmendar Reddy Yanala and Shankar Goud. B [23].

Motivated by the above studies and applications, the present work examines the effect of thermal radiation and chemical reaction on MHD heat and mass transfer Casson Nanofluid flow through a elongating sheet with heat source/sink. This consideration has an important value in engineering and biological research.

MATHEMATICAL FORMULATION

We shall contemplate the steady two-dimensional boundary layer non-Newtonian Casson nanofluid flow past a stretching sheet fixed in a porous medium. The sheet is extending through x -axis with linear velocity $U_w = ax$ at $y = 0$, where a is a positive constant. A constant magnetic flux is oriented perpendicular to the stretching sheet, as shown in Figure-1. Further, it is assumed that at stretching plate temperature T_w and nanoparticle volume fraction C_w and at free stream temperature T_∞ and nanoparticle volume fraction C_∞.

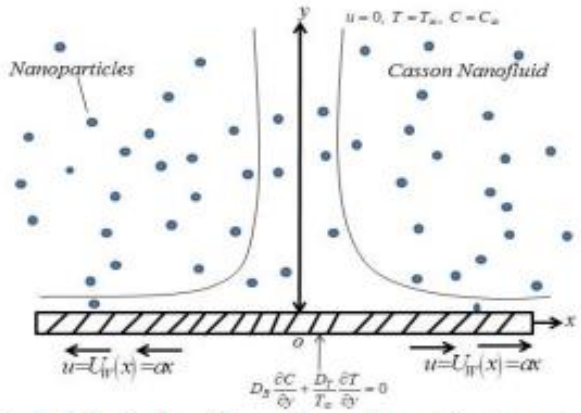

Fig. 1. Physical configuration and coordinate system

The governing equations of boundary layer flow are given by

$$\frac{\partial u}{\partial x} + \frac{\partial v}{\partial y} = 0 \quad (1)$$

$$u\frac{\partial u}{\partial x} + v\frac{\partial u}{\partial y} = \nu\left(1 + \frac{1}{\beta}\right)\frac{\partial^2 u}{\partial y^2} - \frac{\sigma B_0^2}{\rho}u - \frac{\nu}{k_1}u \quad (2)$$

$$u\frac{\partial T}{\partial x} + v\frac{\partial T}{\partial y} = \alpha\frac{\partial^2 T}{\partial y^2} + \tau\left[D_B\frac{\partial C}{\partial y}\frac{\partial T}{\partial y} + \frac{D_T}{T_\infty}\left(\frac{\partial T}{\partial y}\right)^2\right] - \frac{1}{(\rho C_p)_{nf}}\frac{\partial q_r}{\partial y} + \frac{Q_0}{(\rho C_p)_{nf}}(T - T_\infty) \quad (3)$$

$$u\frac{\partial C}{\partial x} + v\frac{\partial C}{\partial y} = D_B\frac{\partial^2 C}{\partial y^2} + \frac{D_T}{T_\infty}\frac{\partial^2 T}{\partial y^2} - K_R(C_R - C_\infty) \quad (4)$$

Where u and v are the velocity profiles along x and y coordinates, ρ_f is the density of the base fluid, , T_∞ is constant temperature of the fluid in the inviscid free stream, ν is the kinematic viscosity, α is the thermal conductivity, $(\rho c)_f$ is the heat capacity of the base fluid, c_p is the specific heat at constant pressure, $(\rho c)_p$ is the effective heat capacity of nanoparticles, D_T is the Thermophoretic diffusion coefficient, D_B is the Brownian diffusion coefficient, K_1 is the permeability of the porous medium, C is nanoparticle volume fraction and T is the temperature

Subject to boundary conditions as

$$u = U_w(x) = ax, v = 0 \;\; T = T_w, D_B\frac{\partial C}{\partial y} + \frac{D_T}{T_\infty}\frac{\partial T}{\partial y} = 0 \text{ at } y = 0 \quad (5)$$
$$u \to 0, \;\; v \to 0 \quad T \to T_\infty, C \to C_\infty \; as \; y \to \infty$$

According to Rosseland's approximation, the radiative heat flux is simplified as

$$q_r = -\frac{4\sigma^*}{3k^*}\frac{\partial T^4}{\partial y} \quad (6)$$

Here the mean absorption and Stefan-Boltzmann coefficient are denoted by k^* and σ^*. By using Taylor series, we can express T^4 in powers of $(T - T_\infty)$ and neglecting the higher order terms, we get

$$T^4 \approx 4T_\infty^3 T - 3T_\infty^4. \quad (7)$$

Using equations (6) and (7), equation (3) becomes

$$u\frac{\partial T}{\partial x} + v\frac{\partial T}{\partial y} = \alpha\,\frac{\partial^2 T}{\partial y^2} + \tau\left[D_B\,\frac{\partial C}{\partial y}\frac{\partial T}{\partial y} + \frac{D_T}{T_\infty}\left(\frac{\partial T}{\partial y}\right)^2\right] + \frac{16\sigma^* T_\infty^3}{3K^*(\rho C_P)_f}\frac{\partial^2 T}{\partial y^2} + \frac{Q_0}{(\rho C_p)_{nf}}(T - T_\infty) \quad (8)$$

The similarity transformations are assumed as

$$\Psi = (av)^{\frac{1}{2}}\,x f(\eta),\quad \eta = \left(\frac{a}{v}\right)^{\frac{1}{2}} y,\ \theta(\eta) = \frac{T - T_\infty}{T_w - T_\infty},\ \emptyset(\eta) = \frac{C - C_\infty}{C_w - C_\infty}. \quad (9)$$

The stream function ψ is interpreted as $u = \frac{\partial \psi}{\partial y}$ and $v = -\frac{\partial \psi}{\partial x}$. Using (9), The equations (2), (4) and (8) are obtained as follows:

$$\left(\frac{1+\beta}{\beta}\right) f''' + f\,f'' - (f')^2 - (M + K)f' = 0 \quad (10)$$

$$\frac{1}{Pr}\left(1 + \frac{4R}{3}\right)\theta'' + Nb\,\theta'\emptyset' + Nt(\theta')^2 + f\theta' + S\theta = 0 \quad (11)$$

$$\emptyset'' + Sc(f\emptyset' - \gamma\emptyset) + \frac{Nt}{Nb}\theta'' = 0 \quad (12)$$

where $M = \frac{\sigma}{\rho a}B_0^2$ Magnetic parameter, $K = \frac{v}{K_1 a}$ porous medium, $R = \frac{4\sigma * T_\infty^3}{K^* K}$ radiation parameter, $Pr = \frac{v}{\alpha}$ Prandtl number, $Nb = \frac{(\rho c)_P D_B (C_w - C_\infty)}{(\rho c)_f v}$ Brownian motion parameter , $Nt = \frac{(\rho c)_P D_T (T_w - T_\infty)}{(\rho c)_f\, v\, T_\infty}$ Thermophoresis parameter, and $Sc = \frac{v}{D}$ Schmidt number, $S = \frac{Q_0}{a\rho c_p}$ heat source/sink parameter, $\gamma = \frac{K_R}{a}$ non-dimensional chemical reaction parameter and $f, \theta, \emptyset$ are function of η and derivative with respective to η is denoted by prime.

The boundary conditions (4), will modify as follows:

$$f(\eta) = 0,\ f'(\eta) = 1,\ \theta(\eta) = 1,\ \emptyset(\eta) = 1 \text{ at } \eta = 0$$
$$f'(\eta) \to 0,\ \theta(\eta) \to 0,\ \emptyset(\eta) \to 0 \text{ as } \eta \to \infty \quad (13)$$

The fascinate of physical quantities are skin friction coefficient C_f, Sherwood number Sh_x and local Nusselt number Nu_x which are defined as

$$C_f = \frac{\tau_w}{\rho\, U_w^2},\quad Sh_x = \frac{x q_m}{D_B(C_w - C_\infty)} and \quad Nu_x = \frac{x\, q_w}{k\, T_\infty} \quad (14)$$

Whereas the shear stress τ_w, surface mass flux q_m and surface heat flux q_w are given by

$$\tau_w = \mu\left(\frac{\partial u}{\partial y}\right), q_m = -D_B\frac{\partial C}{\partial y} \text{ and } q_w = -k\frac{\partial T}{\partial y} \text{ at } y = 0. \quad (15)$$

Utilising the equation (8), we obtain

$$C_f(Re_x)^{\frac{1}{2}} = f''(0),\ \frac{Nu_x}{(Re_x)^{\frac{1}{2}}} = -\theta'(0) \text{ and } \frac{Sh_x}{(Re_x)^{\frac{1}{2}}} = -\emptyset'(0) \quad (16)$$

Where $Re_x = \frac{x\, U_w(x)}{v}$ defined as local Reynold's number.

NUMERICAL PROCEDURE

The differential equations (10)-(12) are highly non-linear and the resulting governing equations subject to the conditions (13) are solved numerically by Keller box technique. The key procedure of Keller box method to find solutions of governing equations as given below:

a) Transformed the given ODE's to a set of the first order equations;

b) Now, Express ODE's in terms of finite differences.

c) The obtained difference equations are linearized with Newton's method and arrange in vector notation.

d) The set of linear equations are solved by the block tridiagonal elimination method.

In this study a uniform mesh of size $\Delta\eta = 0.01$ is taken and the solutions with an error of 10^{-5} obtained in all cases, which provide four decimal places to most of the prescribed values, as shown in tables. The below initial approximations are picked in such a way that to meet the convergence criteria and to satisfies the boundary conditions (13), these guesses can improve the accuracy of the method.

$$f(\eta) = 1 - e^{-\eta},\ \theta(\eta) = e^{-\eta},\ \emptyset(\eta) = e^{-\eta}, \quad (17)$$

RESULTS AND DISCUSSIONS

The differential equations (10)-(12) along with the boundary conditions (13) are evaluated with the help of Keller box method. The fluid velocity, temperature and nanoparticle volume fraction for several values of the pertinent flow constraints viz., Casson parameter β, Nb, Brownian motion parameter, S, Heat Source/Sink, Nt, Thermophoresis parameter, Pr, Prandtl number, M, Magnetic field, R, Radiation parameter, Chemical reaction γ and K porosity parameter, are investigated and displayed in Figures 2-13. The effect of the above parameters on the coefficient of skin friction, Nusselt, and Sherwood number is displayed in Tables 1-2. The accuracy of results is compared and are identified as excellent agreement with results of Yap Bing Kho *et al*. [14].

We observed and confident that by neglecting the impact of K, M, R, S, C_R, Nb and Nt for every value of Pr,

the obtained values of reduced Nusselt number $-\theta'(0)$ are coincide with the results of Yap Bing Kho et al. [14], are shown in Table-1.

Table-1. Comparison of results for the local Nusselt number $-\theta'(0)$ when $\beta = \infty, Sc = 1, R = Nb = Nt = S = C_R = K = M = 0$.

Pr	Local Nusselt number $-\theta'(0)$	
	Yap Bing Kho [14]	**Present Study**
0.20	0.1698	0.1697
0.70	0.4539	0.4544
2.00	0.9113	0.9113
7.00	1.8954	1.8954
20.00	3.3539	3.3541

Table-2 exhibits numerical calculations for various values of M, C_R, S, R, Nb, Nt, Sc and β when Pr = 0.72, K = 0.3. As the magnetic field M enhances, the obtained values indicate the rise in the local skin friction coefficient $f''(0)$, local Nusselt and Sherwood numbers $(-\theta'(0), -\phi'(0))$. Both local Nusselt number $-\theta'(0)$ and local Sherwood number $--\phi'(0)$ are rises as Chemical reaction (C_R) and Schmidt number increases. As Heat Source/ Sink (S) and Radiation parameter (R) increases, Nusselt number diminishes and Sherwood number enhances. As Thermophoresis parameter (Nt) and Brownian motion parameter (Nb) increases, the Nusselt number reduces and Sherwood number hikes. As Casson parameter β increases, skin friction coefficient and Sherwood number enhances, local Nusselt number decreases.

Table-2. Numerical values of local skin friction coefficient $f''(0)$, local Nusselt number $-\theta'(0)$ and local Sherwood number $-\phi'(0)$ for different values of M, C_R, S, R, Nb, Nt, Sc and β when Pr = 0.72, K = 0.3.

M	C_R	S	R	β	Nb	Nt	Sc	$f''(0)$	$-\theta'(0)$	$-\phi'(0)$
0.1	**0.2**	**0.5**	**0.25**	**0.5**	**0.3**	**0.1**	**0.1**	**0.6831**	**0.1583**	**0.1833**
0.2								0.7071	0.3913	0.2549
0.3								0.7303	0.5002	0.3738
0.5	0.5							0.7746	0.6656	- 4.319
	1.0							0.7746	0.8853	0.1870
	1.5							0.7746	0.9094	0.2736
		0.5						0.7746	0.8231	0.0184
		1.0						0.7746	0.4969	0.0804
		2.0						0.7746	0.2008	0.3022
			1					0.7746	0.1897	0.1674
			2					0.7746	0.0232	0.2130
			4					0.7746	0.0211	0.2226
				0.5				0.7746	1.8231	0.0184
				1.0				0.9487	1.2455	0.0217
				1.5				1.0392	0.8316	0.0365
					0.1			0.7746	0.8831	0.5007
					0.2			0.7746	0.8522	0.6385
					0.3			0.7746	0.8231	0.7184
						0.1		0.7746	0.8231	0.0184
						0.2		0.7746	0.8064	0.2215
						0.3		0.7746	0.7903	0.4147
							0.2	0.7746	0.8747	0.0958
							0.3	0.7746	0.9194	0.1868
							0.4	0.7746	0.9574	0.2654

The dimensionless velocity and temperature fields are plotted in Figures 2 & 3 for different values of Casson parameter β. It reveals that the velocity diminishes and temperature hikes as Casson parameter enhances. Yield stress reduces while an increase in β, works like Newtonian fluid ($\beta \to \infty$).

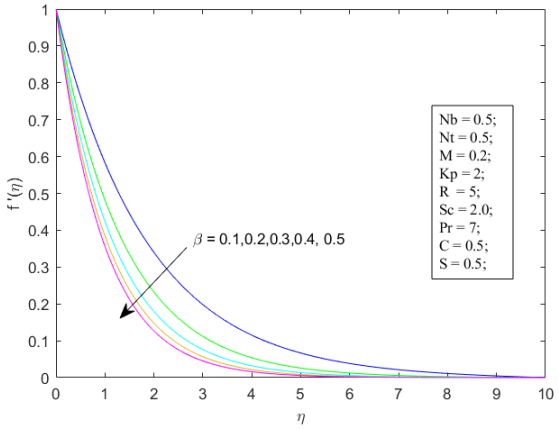

Figure 2: Velocity profile for various values of casson parameter(β)

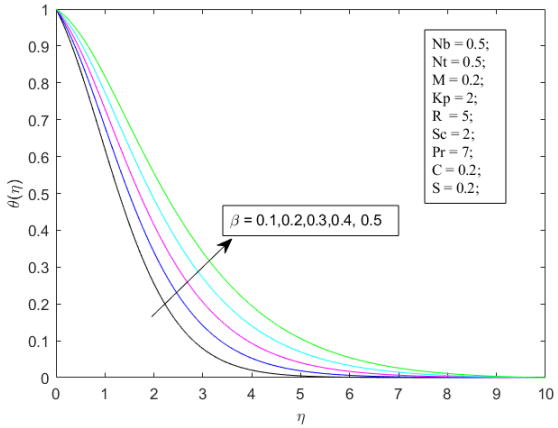

Figure 3: Temerature profile for various values of casson parameter (β)

Figures 4 & 5 depict the impact of magnetic field M on velocity and temperature distributions, As M rises the velocity drops. Geometrically, the reason for the slowdown in velocity on the surface due to the fact that the fluid movement occurs as a result of stretching of the surface, which is limited due to application of a magnetic field, since the magnetic field creates resistance force, namely the Lorentz force, which slow down the fluid motion. Figure-5 displayed that magnetic field boosting the temperature profile of the fluid flow.

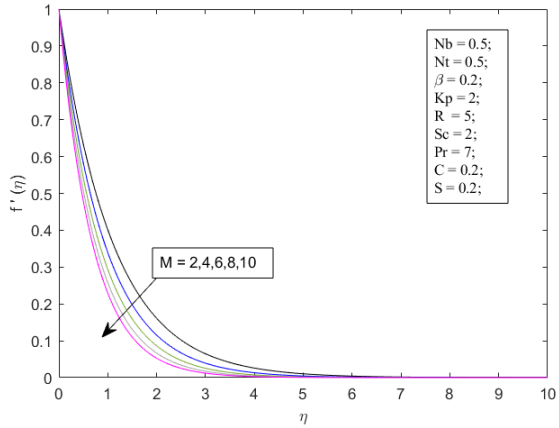

Figure 4: Velocity profile for various values of Magnetic parameter (M)

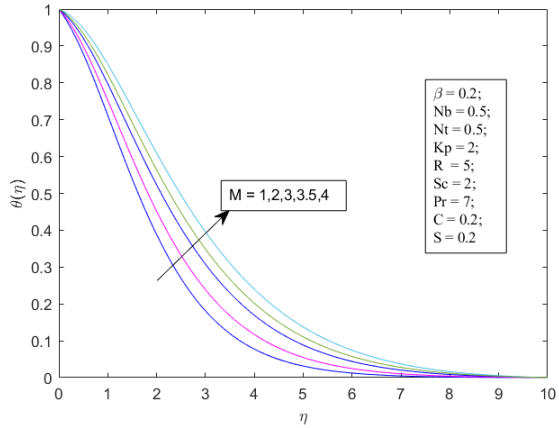

Figure 5: Temperature profile for various values of Magnetic parameter (M)

Figures 6 and 7 illustrate the thermal and nanoparticle concentration distribution for different values of Brownian motion parameter Nb. It is noted that an escalation in the Brownian motion Nb causes a rise in the dimensionless temperature, but the reverse trend is observed for nanoparticle concentration. Movement of particles is known as Brownian motion and the agile motion of the particles generates more heat and hence rises in temperature.

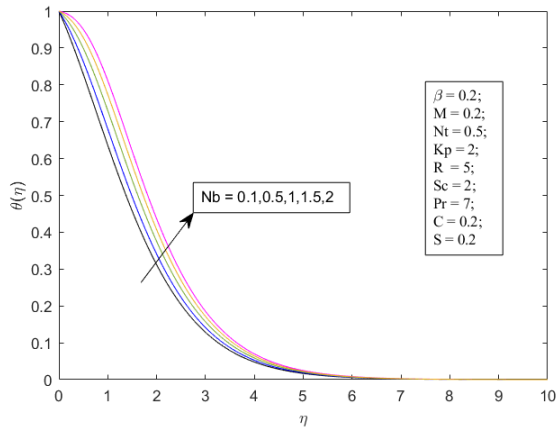

Figure 6: Temperature profile for various values of Brownian motion parameter Nb

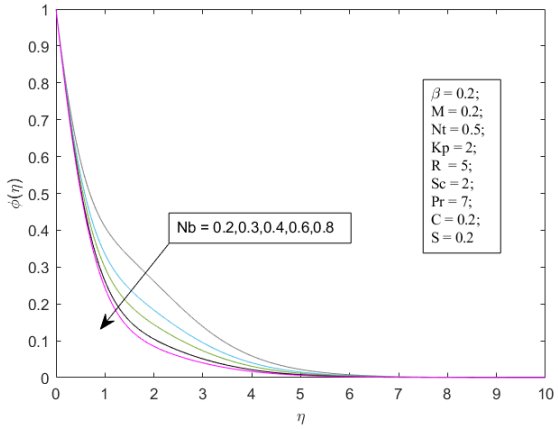

Figure 7: Concentration profile for various values of Brownian motion parameter Nb

Figures 8 & 9 show the influence of the Nt on dimensionless temperature and concentration. It is noted that, a growth in the value of Nt led to an escalation in temperature and concentration. In Figure 10, the result shown that the R value increases, so the dimensionless temperature also increases.

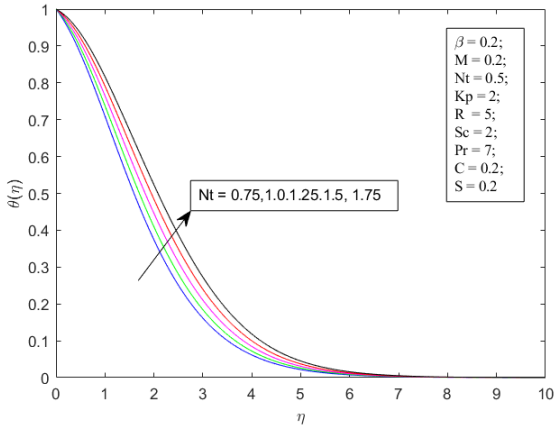

Figure 8: Temperature profile for various values of thermoporesis parameter Nt

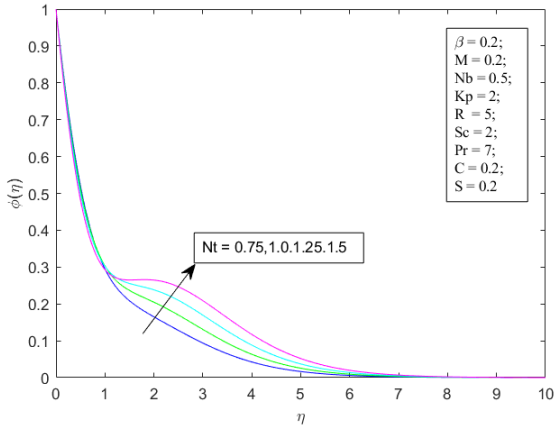

Figure 9: Concentration profile for various values of thermoporesis parameter Nt

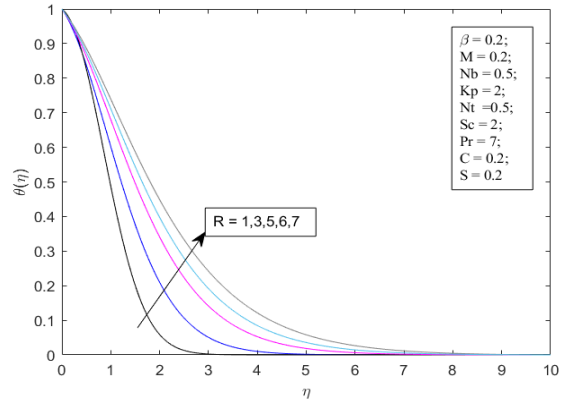

Figure 10: Temperature profile for various values of Radiation parameter R

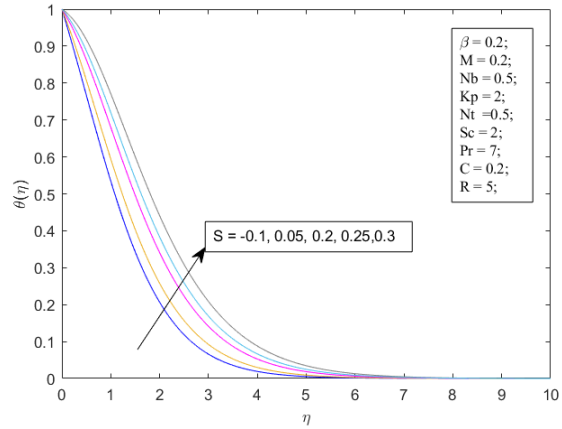

Figure 11: Temperature profile for various values of Heat source/ sink (S)

Figure-11 shows that the temperature θ (η) increases with an increase in the resistance of the heat source / sink, due to an increase in the resistance of the heat generation, the temperature rises. Figure-12 portraits the effect of chemical reaction parameter C_R on nanoparticle volume fraction. It is found that concentration decreases as the chemical reaction C_R increases.

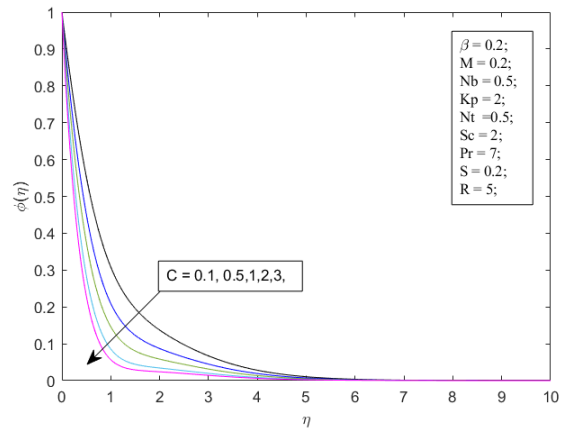

Figure 12:Concentration profile for various values of Chemical reaction parameter (C

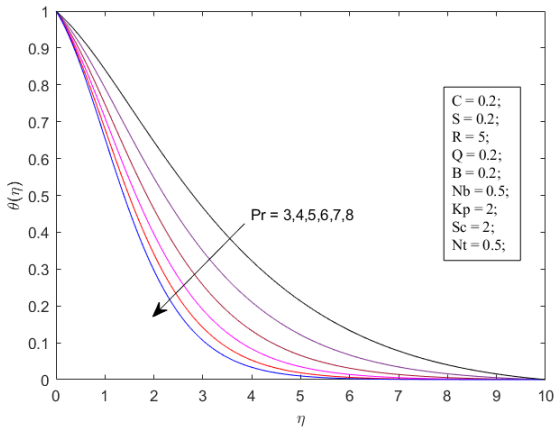

Figure 13: Temperature profile for various values of prandtl number (Pr)

The temperature field for different values of the Prandtl number Pr is presented in Figure-13. The dimensionless temperature profile decreases with an increasing value of Pr. An increase in Prandtl number means a decrease in the thermal conductivity of the fluid, causing a decrease in temperature.

CONCLUSIONS

Impact of thermal radiation on MHD Casson nanofluid flow along a stretching sheet with chemical reaction and heat generation/absorption effects. The Keller-Box method is used to solve the resulting set of non-linear ODE's with boundary conditions. The influence of Casson, chemical reaction, Thermophoresis, magnetic, Brownian motion, Heat Source/ Sink, thermal radiation parameters, Schmidt and Prandtl number are analysed and presented graphically. The current study gives the conclusions as follows:

a) An enhance in magnetic field M and β, the dimensionless velocity drops where as reverse trend is observed in the temperature profile.

b) It is noted that nanoparticle temperature accelerates and reduction in concentration distribution for several value of Nb.

c) The thermophoresis parameter Nt improves the thermal and concentration profiles.

d) Higher values of R and S are responsible for increase in the temperature profile.

e) Concentration profile decreases as the chemical reaction C_R increases.

f) Rising values of Pr, reduces the thermal boundary layer and the rate of heat transfer $-\theta'(0)$.

g) An increase in Magnetic parameter (M) and Casson parameter (β) enhances Skin-friction coefficient $f''(0)$, heat and mass transfer rates.

h) An increase in Chemical reaction (C_R), Schmidt number (Sc), there is an enhancement in local Nusselt and Sherwood numbers.

i) As increase of Heat absorption/generation (S) and thermal radiation (R), reduces the heat transfer rate $-\theta'(0)$ and enhances the mass transfer rate $-\phi'(0)$.

REFERENCES

[1] Stephen U. S. Choi and J. A. Eastman. Enhancing thermal conductivity of fluids with nanoparticles, developments and applications of non-Newtonian flows, ANL/MSD/CP-84938; CONF-951135-29.

[2] S. K. DAS *et al.* 2006. Heat Transfer in Nanofluids, Heat Transfer Engineering. 27(10): 3-19.

[3] A. Aziz and W. A. Khan. 2012. Natural convective boundary layer flow of a nanofluid past a convectively heated vertical plate. International Journal of Thermal Sciences. 52: 83-90.

[4] D. Srinivasacharya and Ontela Surender. 2014. Non-similar solution for natural convective boundary layer flow of a nanofluid past a vertical plate embedded in a doubly stratified porous medium. International Journal of Heat and Mass Transfer. 71: 431-438.

[5] A. H. Elsheikh *et al.* 2018. Applications of nanofluids in solar energy: A review of recent advances, Renewable and Sustainable Energy Reviews. 82: 3483-3502.

[6] Rizwan Ul Haq *et al.* 2015. Thermal radiation and slip effects on MHD stagnation point flow of nanofluid over a stretching sheet, Physica: E 65: 17-23.

[7] A. S. Dogonchi *et al.* 2016. Flow and heat transfer of MHD nanofluid between parallel plates in the presence of thermal radiation, Comput. Methods Appl. Mech. Engrg. S0045-7825: 30288-2.

[8] A. Kamran *et al.* 2017. A numerical study of magnetohydrodynamics flow in Casson nanofluid combined with Joule heating and slip boundary conditions. Results in Physics. 7: 3037-3048.

[9] Jawad Raza *et al*. 2019. Multiple slip effects on MHD non-Newtonian nanofluid flow over a nonlinear permeable elongated sheet Numerical and statistical analysis Multidiscipline Modeling in Materials and Structures. 15(5): 913-931.

[10] Saeed Islam *et al*. 2020. Influences of Hall current and radiation on MHD micropolar non-Newtonian hybrid nanofluid flow between two surfaces. AIP Advances. 10, 055015.

[11] Yanala Dharmendar Reddy *et al*. 2016. Effect of Thermal Radiation on MHD Boundary Layer Flow of Nanofluid and Heat Transfer Over a Non-Linearly Stretching Sheet with Transpiration. Journal of Nanofluids. 5-6: 889-897.

[12] M. Kothandapani and J. Prakash. 2015. Effects of thermal radiation parameter and magnetic field on the peristaltic motion of Williamson nanofluids in a tapered asymmetric channel, International Journal of Heat and Mass Transfer. 81: 234-245.

[13] C. Sulochana *et al*. 2016. Thermal radiation effect on MHD nanofluid flow over a stretching sheet. International Journal of Engineering Research in Africa. 23: 89-102.

[14] Yap Bing Kho *et al.* 2018. Thermal Radiation Effects on MHD with Flow Heat and Mass Transfer in Casson Nanofluid over a Stretching Sheet. MATEC Web of Conferences 150, 06036.

[15] Jawad Raza. 2019. Thermal radiation and slip effects on magnetohydrodynamic (MHD) stagnation point flow of Casson fluid over a convective stretching sheet. Propulsion and Power Research. 8(2): 138-146.

[16] Manjula Jonnadula *et al*. 2015. Influence of Thermal Radiation and Chemical Reaction on MHD Flow, Heat and Mass Transfer over a Stretching Surface, Procedia Engineering. 127: 1315-1322.

[17] Tasawar Hayat *et al*. 2015. Magnetohydrodynamic (MHD) stretched flow of nanofluid with power-law velocity and chemical reaction. AIP Advances. 5, 117121.

[18] N. Pandya *et al*. 2017. Combined effects of Soret-Dufour, Radiation and Chemical reaction on Unsteady MHD flow of Dusty fluid over inclined porous plate embedded in porous medium. Int. J. Adv. Appl. Math. and Mech. 5(1): 49-58 (ISSN: 2347-2529).

[19] Sajid Qayyum at al. 2017. Effect of a chemical reaction on magnetohydrodynamic (MHD) stagnation point flow of Walters-B nanofluid with Newtonian heat and mass conditions. Nuclear Engineering and Technology. 49: 1636-1644.

[20] G. Sreedhar and B. Rama Bhupal Reddy. 2019. Chemical Reaction Effect on Unsteady MHD Flow Past an Infinite Vertical Porous Plate in The Presence of Heat Absorption. International Journal of Advanced Research in Engineering and Technology. 10: 95-103.

[21] Dileep Kumar and A. K. Singh. 2016. Effects of heat source/sink and induced magnetic field on natural convective flow in vertical concentric annuli. Alexandria Engineering Journal. 55: 3125-3133.

[22] Rafael Cortell Bataller. 2007. Effects of heat source/sink, radiation and work done by deformation on flow and heat transfer of a viscoelastic fluid over a stretching sheet. Computers and Mathematics with Applications. 53: 305-316.

[23] Dharmendar Reddy and Yanala Shankar Goud.B. 2020. Heat Source Effect on MHD Fluid Flow Over a Moving Vertical Plate in the presence of Chemical Reaction with Convective surface Boundary Conditions. Journal of Engineering, Computing and Architecture. 10-1: 38-46.